



Contents lists available at ScienceDirect

## Physics of the Earth and Planetary Interiors

journal homepage: [www.elsevier.com/locate/pepi](http://www.elsevier.com/locate/pepi)



### Seismic attenuation in a phase change coexistence loop

Yanick Ricard\*, J. Matas, F. Chambat

Laboratoire des Sciences de la Terre, CNRS, Université de Lyon, Bat Géode, 2 rue Raphael Dubois, 69622, Villeurbanne, 07, France

#### ARTICLE INFO

##### Article history:

Received 26 November 2008  
Received in revised form 18 April 2009  
Accepted 29 April 2009

##### Keywords:

Seismic attenuation  
Phase change

#### ABSTRACT

Most phase transformations in the mantle occur across regions of multi-phase coexistence. Inside these regions, the long-term incompressibility becomes very low because the density can increase both by compression and by changing phase. This difference between long-term and elastic incompressibilities is a typical situation where seismic attenuation may happen. In this paper, we discuss the various differences between the classical theory of sound attenuation in a reacting fluid and the case of seismic propagation in a two-phase loop. We derive a simple analytical model of a two-phase loop to show that the phase change should affect both the bulk and the shear attenuation and in rather similar proportion. We show that attenuation occurs over two different frequency ranges. For the olivine–wadsleyite phase change, the low frequency attenuation occurs for periods larger than hundreds of years but the high frequency band occurs between 1 min and 1 h (from 16 to 0.27 mHz) in the domain of surface waves and seismic modes. We predict both bulk and shear quality factors between 1 and 10 in the middle of the 410 km phase loop.

© 2009 Elsevier B.V. All rights reserved.

The response to stress changes of the mineral aggregate that constitutes the mantle controls the velocity and dissipation of seismic waves. As it is generally easier to work with arrival times or velocities of seismic waves than with their amplitudes, the seismologists have made more remarkable progress in mapping radial or 3D velocity structures than in mapping the attenuation. The scattering of seismic waves by small scale heterogeneities and the focussing–defocussing effects of wave propagation in the presence of 3D velocity structures are indeed difficult to separate from intrinsic attenuation. In spite of observational difficulties, several global models of 1D attenuation have however been published (e.g., [Dziewonski and Anderson, 1981](#); [Widmer et al., 1991](#); [Durek and Ekstrom, 1996](#)). The disagreement between them is however large and often larger than the uncertainties suggested by each individual model (see e.g., [Romanowicz and Mitchell, 2007](#), for a discussion). Three dimensional models are also available but are still a challenge and only the structures of the largest wavelengths have been mapped ([Gung and Romanowicz, 2004](#)). A better knowledge of attenuation is necessary to interpret the tomographic images and would however significantly improve our knowledge of mantle temperature ([Anderson and Given, 1982](#); [Karato and Karki, 2001](#); [Matas and Bukowski, 2007](#); [Brodholt et al., 2007](#); [Lekić et al., 2009](#)).

In the last 40 years (e.g., [Jackson and Anderson, 1970](#); [Anderson, 1976](#); [Karato and Spetzler, 1990](#)), various attenuation mechanisms

have been discussed including those due to phase changes. The attenuation of sound in a media undergoing a phase change is indeed a classical example of irreversible process that leads to attenuation ([de Groot and Mazur, 1984](#)). Recently [Li and Weidner \(2008\)](#) have succeeded in the very difficult laboratory measurement of attenuation that takes place across the mantle transition zone, due to the presence of phase changes. Their paper assumes that the phase change attenuation is only related to compression, i.e., to what seismologists call the “bulk attenuation” (the quantity of energy lost during an oscillation of a pure isotropic compression). This attenuation is accounted for by the quality factor  $Q_K$  on which seismologists have very little resolution. Seismologists tend to ascribe most of the attenuation to the “shear attenuation” accounted for by the quality factor  $Q_\mu$ .

In the laboratory, the pressure changes used to drive the phase change are at the gigapascal level, while those due to seismic wave propagation are much smaller, typically of order  $10^{-7}$  GPa (e.g., [Aki and Richards, 2002](#)). To rescale their observations, [Li and Weidner \(2008\)](#) propose a qualitative model of attenuation where the pressure perturbation  $\delta P$  associated with the seismic wave would drive the phase change at the interface between two grains by a distance  $d \propto \delta P$  and this length should be compared to the time  $t$  necessary for cation diffusion, with  $t \propto d^2$ . Their model suggests therefore that the attenuation and the relaxation times are related to the amplitude of the seismic perturbation. This non-linearity would invalidate various assumptions of seismology, like the principle of linear superposition or the ability to describe the wavefield observation of an instrument as a series of convolutions. It would imply that seismic waves from large

\* Corresponding author.

E-mail address: [yanick.ricard@ens-lyon.fr](mailto:yanick.ricard@ens-lyon.fr) (Y. Ricard).

earthquakes see a more attenuating mantle than those from small ones.

The model of Li and Weidner (2008) is based on general considerations that are explained in more details in Jackson (2007). However, Jackson (2007) warns us that “no attempt has been made to model the time-dependent stress at the phase boundary or the transformation kinetics, potentially strongly influenced by the rheology of the surrounding medium”. This is what we do in this paper where we propose a micro-mechanical model of a coexistence loop. We show that dissipation occurs in two different time periods and that the resulting attenuations are independent of the seismic wave amplitudes. We confirm that phase change loops may be the zones of large attenuations. We show that they should affect rather similarly the compressibility and the shear modulus.

## 1. Reaction rates of phase changes

The mechanism of attenuation due to a phase change in the mantle (or in a fluid) is easy to understand (de Groot and Mazur, 1984). The changes of pressure due to a propagating sound wave affect differently the chemical potentials of the various coexisting phases and thus modify locally the thermodynamic equilibrium. This drives a mineralogical phase change, a possible source of dissipation. However, the theory of seismic attenuation in the mantle cannot be directly derived from that of sound attenuation in fluids because the physics differs by at least four aspects.

- First, the propagation of elastic waves is related to the rigidity  $\mu$  (entirely for the S waves, and partly for the P waves) which is not considered for sound wave attenuation in fluids.
- Second, contrary to gases or fluids that are usually used in textbooks to illustrate thermodynamics, the thermodynamic equilibrium in complex solid aggregates is related to stresses, not to pressure. The pressure is not a continuous quantity across the grain interfaces. According to Shimizu (1997), a chemical potential tensor should be defined on interfaces and the reaction rate should also depend on the crystal orientation. We assume here that the equilibrium on an interface only depends on the stresses normal to this interface  $\sigma_n$  which is a continuous variable (Paterson, 1973). In the absence of any viscoelastic stresses, the normal stress and the pressure can be identified and the usual thermodynamic rules are recovered.
- Third, the rheology of the mantle is not only simply elastic but viscoelastic. Deviatoric stresses can relax for times larger than the Maxwell time of the viscoelastic mantle, the ratio of viscosity to rigidity (see e.g., Ricard, 2007).
- Fourth, the phase transformations in the mantle are not univariant. As mantle materials are solid solutions and involves various cations, the phase changes occur across phase loops where two of more phases of various compositions coexist. For example, around 410 km, an olivine with a Fe/Mg ratio typically of 1/10 (Ringwood, 1982), enters a phase loop where wadsleyite, with a larger Fe/Mg ratio, nucleates and then grows. This larger ratio is balanced by a symmetrical decrease of the Fe/Mg ratio in the remaining olivine. Across the phase loop the percentage of wadsleyite increases with depth and this wadsleyite has a decreasing Fe/Mg ratio until the ratio of 1/10 which corresponds to the disappearance of the last grains of olivine. Notice that in a phase loop, the two phases are already present and the nucleation of new grains should not control the kinetics of transformation, contrary to what may happen when a single phase moves through a phase transition (Rubie and Ross, 1994).

The sound propagation theory shows that the attenuation is ultimately related to the difference between the elastic parameters at very high frequency (the unrelaxed parameters) and those at very low frequency (the relaxed parameters) if the relaxation occurs within the period of the sound wave. The time dependent pressure variations  $\delta P(t)$  due a high frequency seismic body wave, and the associated density variations  $\delta\rho(t)$  are related by

$$\delta P(t) = \kappa_\infty \frac{\delta\rho(t)}{\rho}, \quad (1)$$

where  $\kappa_\infty$  is the elastic incompressibility (or elastic bulk modulus). The subscript  $\infty$  indicates that this corresponds to the limit of infinite frequency,  $\omega = +\infty$ . More precisely,  $\kappa_\infty$  should be the isentropic incompressibility  $\kappa_S$  but we will not distinguish in this paper between the isothermal and isentropic elastic incompressibilities,  $\kappa_T$  and  $\kappa_S$ , that are at any rate, equal within 1%.

At thermodynamic equilibrium, inside a multi-phase loop where the density jumps by  $\Delta\rho$  over a depth range  $\Delta P$ , depth dependent pressure variations and depth dependent density variations are roughly proportional and related by

$$\frac{dP}{dr} = \frac{\kappa_0}{\rho} \frac{d\rho}{dr} \quad \text{with} \quad \kappa_0 = \rho \frac{\Delta P}{\Delta\rho}. \quad (2)$$

The equilibrium relation (2) defines the relaxed bulk modulus in the limit of zero frequency (see also, Jacobs and de Jong, 2005).

If we take the example of the phase change around 410 km depth, between olivine and wadsleyite, the unrelaxed incompressibility (elastic bulk modulus) is around  $\kappa_\infty = 180$  GPa. With an average density of  $3630 \text{ kg m}^{-3}$  and a density jump of  $180 \text{ kg m}^{-3}$  over a thickness of 10 km (this value is reasonable although estimates ranging from 5 to 30 km have been proposed (see e.g., Shearer, 2000; Van der Meijde et al., 2003; Ricard et al., 2005)), the relaxed incompressibility is  $\kappa_0 = 7$  GPa. Outside a coexistence loop, the elastic incompressibility  $\kappa_\infty$  that can be measured by a time dependent phenomenon (the propagation of elastic waves) and the incompressibility measured along a radial profile  $\kappa_0$  are usually considered as equal (or at least very close, see e.g., Bullen, 1940).

The numerical expression of  $\kappa_0$  in Eq. (2) can be expressed in a more physical way that demonstrates that  $\kappa_0$  is bounded by  $\kappa_\infty$  (Li and Weidner, 2008). The density jump across a phase change  $\Delta\rho$  is due both to an intrinsic density jump  $\Delta\rho_\chi$  (the density difference between the two phases at a given pressure and temperature) and to the compression of the material across the coexistence loop. In other term, the relaxed compressibility in the phase loop,  $1/\kappa_0$ , is due both to the elastic compressibility  $1/\kappa_\infty$  and to an apparent compressibility to the density jump  $\Delta\rho_\chi$  existing between the two phases so that

$$\frac{1}{\kappa_0} = \frac{1}{\kappa_\infty} + \frac{\Delta\rho_\chi}{\rho} \frac{1}{\Delta P} > \frac{1}{\kappa_\infty}. \quad (3)$$

When the transition thickness becomes very large,  $\kappa_\infty$  and  $\kappa_0$  become therefore equal.

The evolution of an interface interacting with an elastic wave can be computed from the mechanical properties of the two phases and the boundary conditions on the interface. At the interface between grains, the total normal stress (pressure plus deviatoric stress) and shear stress are continuous. The boundary condition for the velocity across the reacting interface is expressed by

$$\rho_\alpha(\mathbf{v}_\alpha - \mathbf{V}) \cdot \mathbf{n} = \rho_\beta(\mathbf{v}_\beta - \mathbf{V}) \cdot \mathbf{n} = -\Delta\Gamma, \quad (4)$$

where  $\rho_i$  and  $\mathbf{V}_i$  are the densities and the velocities of each phase,  $\mathbf{n}$  the normal to the interface of the two media, directed from  $\alpha$  to  $\beta$ ,  $\mathbf{V}$  the interface velocity and  $\Delta\Gamma$  the reaction rate of the  $\alpha \rightarrow \beta$  reaction (in  $\text{kg m}^{-2} \text{ s}^{-1}$ ). The velocity jump across the interface is

therefore

$$(\mathbf{v}_\alpha - \mathbf{v}_\beta) \cdot \mathbf{n} = -\frac{\Delta\rho}{\rho_\alpha\rho_\beta} \Delta\Gamma, \quad (5)$$

where  $\Delta\rho$  stands for  $\rho_\beta - \rho_\alpha$ .

Although the expression of the reaction rate  $\Delta\Gamma$  might be very complex, it must cancel when the two phases are at thermodynamic equilibrium. The definition of the thermodynamic equilibrium is however subtle in the two-phase loop, and we discuss here two possible equilibrium conditions. We show in the following that the choice of one or the other expression does not change our conclusions on the seismic attenuation within the two-phase loop.

When the material inside a phase loop is at equilibrium, the reaction rate is zero. When the system is perturbed, for example by a change of the far-field pressure, the normal stress on interfaces changes. The rules of irreversible thermodynamics (de Groot and Mazur, 1984) suggests that the reaction rate close to equilibrium is proportional to the distance to equilibrium, i.e., to the change of affinity of the reaction.

The associated changes of chemical potentials are initially related to the normal stress perturbations on the grain interfaces  $\delta\sigma_n$ . Therefore the reaction rate has often been chosen in previous modelling to be (e.g., Morris, 2002; Krien and Fleitout, 2008)

$$\Delta\Gamma \propto -\delta\sigma_n \quad (6)$$

(the minus sign comes from the convention sign for normal stress, opposite to pressure, in fluid mechanics). For a very slow perturbation, however, Eq. (6) cannot hold. On a time scale for which inter atomic diffusion occurs, the Fe/Mg content of each phase evolves, and as the chemical potentials are also functions of composition, a new equilibrium is found. The reaction occurs until the pressure change and the density change are related by the condition (2). This implies to choose

$$\Delta\Gamma \propto -\delta\sigma_n - \kappa_0 \frac{\delta\rho}{\rho}. \quad (7)$$

This relation could be rigorously obtained by following the more formal derivation of de Groot and Mazur (1984) provided the pressure replaces the normal stress. As  $\kappa_0$  is very small, we will see that the difference in the attenuation predictions between using (6) or (7) is however only sensible at very long periods, outside the seismic frequency band.

We now need to define the geometrical distribution of the phases inside the loop and use (4) with (6) or (7) to be able to predict the effect of a seismic wave on the interface and thus on the attenuation. We assume that in each half of a phase loop, the minor phase is made of spherical grains surrounded by the major phase (Morris, 2002). For example, in the shallower half of the 410 km depth transition, we consider the  $\beta$ -phase as surrounded by the  $\alpha$  matrix (see Fig. 1). The outer radius  $R_e$  represents the average distance between the grains with radii  $r \leq R_e$  of the minor phase. In the deepest part of the loop, the major  $\beta$ -phase is supposed to surround the last grains of  $\alpha$ -phase. This model will be used to describe the whole loop, although it is obvious that none of the two phases surrounds the other one in the middle of the loop.

When the normal stress on an interface is increased, a new film of the high pressure  $\beta$ -phase grows at the expense of the low pressure  $\alpha$ -phase. This reaction, associated with minor changes of volume, facilitates the deformation, decreases the effective strength, dissipates the elastic energy and therefore leads to attenuation. Notice that with the low pressure changes involved during the propagation of a seismic front,  $\sim 10^{-7}$  GPa, the thickness of the reacting film is only nanometric (Li and Weidner, 2008). This very small perturbation is however a significant source of dissipation.

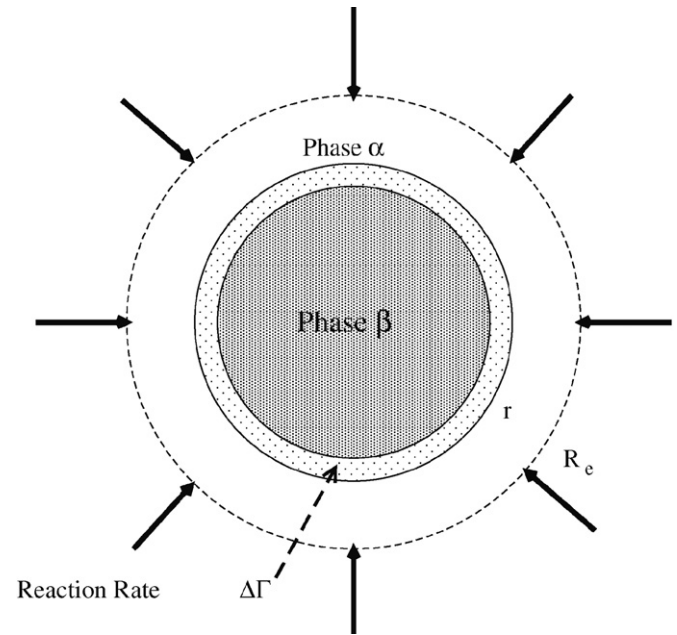


Fig. 1. The growing  $\beta$ -phase is surrounded by the low pressure  $\alpha$ -phase. The interface at radius  $r$  moves up or down depending of the applied external pressure that controls the reaction rate  $\Delta\Gamma$ . The external diameter  $2R_e$  will be interpreted as the average distance between grains.

## 2. Radial deformation and complex incompressibility

We assume for simplicity that the two phases have the same elastic properties with bulk modulus  $\kappa$  and rigidity  $\mu$ . We neglect the difference of these parameters for the two phases which is of the order of the jumps in incompressibility and rigidity, about 10% in PREM, at 410 km depth (Dziewonski and Anderson, 1981). We introduce the normalized radius  $s = r/R_e$  where  $R_e$  is the external radius and we use  $S$  for the value of  $s$  on the two-phase interface.

In the case of isotropic radial compression of the two medium of Fig. 1, it is straightforward to show that with spherical symmetry the radial deformation  $u_r(s)$  in an elastic shell of compressibility  $\kappa_\infty$  and rigidity  $\mu$  can be written

$$u_r^i = a_i s + \frac{b_i}{s^2}, \quad (8)$$

with  $i = \alpha$  in the outer shell and  $i = \beta$ , inside ( $b_\beta$  is obviously 0 to insure that  $u_r^\beta$  is finite at  $s = 0$ ). The change of density is

$$\delta\rho = -3\bar{\rho} \frac{u_r(R_e)}{R_e}, \quad (9)$$

and the effective compressibility of the medium is  $\kappa$ ,

$$\kappa = \bar{\rho} \frac{\delta P}{\delta\rho} = -\frac{R_e}{3u_r(R_e)} \delta P, \quad (10)$$

where  $u_r(R_e)$  and  $\delta P$  are the radial displacement and the pressure perturbation at the outer radius  $R_e$ .

By using the general expression of the jump of normal velocity (5) and one of the kinetic laws (6) and (7), we can write

$$v_\alpha - v_\beta = C \left( \delta\sigma_n(S) - 3\kappa_0 \frac{u(R_e)}{R_e} \right), \quad (11)$$

where  $C$  is a kinetic factor in  $\text{m s}^{-1} \text{Pa}^{-1}$  (the factor  $C$  includes the  $\Delta\rho/\rho_\alpha\rho_\beta$  term of (5)). By choosing a vanishingly small  $\kappa_0$  or the  $\kappa_0$  deduced from the observed thickness of the transition we will be in agreement with (6) or with (7).

If a sinusoidal pressure perturbation of frequency  $\omega$ ,  $\delta P \exp(i\omega t)$ , is applied on the external rim, the deformations and therefore the

coefficients  $a_i$  and  $b_i$ , will also vary at the same frequency. From the general expression of the deformation, (8), the normal stress can be expressed (see Appendix A). By matching the normal stresses across the phase boundary at  $s$  and using the normal velocity jump condition (11) with  $v_\alpha = i\omega u_r^\alpha$  and  $v_\beta = i\omega u_r^\beta$ , the three constants  $a_\alpha$ ,  $b_\alpha$  and  $a_\beta$  can be found from which the effective incompressibility (10) is readily obtained (see Appendix A).

We get

$$\kappa_{HF} = \kappa_\infty + \frac{\kappa_i - \kappa_\infty}{1 + i\omega\tau_1} \quad (12)$$

(HF stands for “high frequency” as it will be explained below) where

$$\kappa_i = \kappa_\infty - S^3(\kappa_\infty - \kappa_0) \frac{\kappa_\infty + 4\mu_\infty/3}{\kappa_\infty S^3 + 4\mu_\infty/3}, \quad (13)$$

and where the relaxation constant  $\tau_1$  is

$$\tau_1 = \frac{R_e S}{3C\kappa_\infty} \frac{\kappa_\infty + 4\mu_\infty/3}{\kappa_\infty S^3 + 4\mu_\infty/3}. \quad (14)$$

The use of the subscripts  $i$  for “intermediate” will soon be explained. The incompressibility at infinite frequency which is usually called the unrelaxed incompressibility is simply the elastic incompressibility  $\kappa_\infty$ , while  $\kappa_i$  is the relaxed incompressibility obtained for  $\omega = 0$ .

It might be surprising that the relaxed incompressibility  $\kappa_i$  in this model does not correspond to the incompressibility  $\kappa_0$  (see (2)) obtained from a radial seismological model. This is because in a purely elastic model, the deviatoric stresses remain in the elastic matrix even at infinite time. To clarify this point we have to remember that at large times, the Earth mantle does not behave as elastic but as viscous. The rigidity in the definition of  $\kappa_i$ , is in fact the high frequency limit of a viscoelastic rheology (see e.g., Ricard, 2007)

$$\mu^* = \mu_\infty \frac{i\omega\tau_M}{1 + i\omega\tau_M}, \quad (15)$$

where  $\tau_M$  is the Maxwell time, ratio of viscosity to rigidity (the real elastic rigidity). If we redo the same modeling using  $\mu^*$  instead of  $\mu_\infty$  we get the same expressions as (12) and (13) but where  $\mu^*$  replaces  $\mu_\infty$ . The new expression of the viscoelastic incompressibility can be simplified and becomes after some algebra

$$\kappa = \kappa_\infty + \frac{\kappa_i - \kappa_\infty}{1 + i\omega\tau_1} + \frac{\kappa_0 - \kappa_i}{(1 + i\omega\tau_1)(1 + i\omega\tau_2)}, \quad (16)$$

with the long relaxation time  $\tau_2$

$$\tau_2 = \tau_M \frac{\kappa S^3 + 4\mu/3}{\kappa S^3}. \quad (17)$$

We can safely assume, at least for the olivine–wadsleyite transformation (see e.g., Li and Weidner, 2008), that  $\tau_1 \ll \tau_2 \sim \tau_M$ , i.e., that the reaction occurs in a time shorter than the Maxwell time of a few hundred years. As is physically expected, the high frequency limit, when  $1 \ll \omega\tau_1 \ll \omega\tau_2$  is the elastic value  $\kappa = \kappa_\infty$  and the low frequency limit  $\omega\tau_1 \ll \omega\tau_2 \ll 1$  is the incompressibility deduced from the thickness of the phase loop,  $\kappa = \kappa_0$ . The incompressibility variations occur within two frequency bands, one for  $\omega\tau_1 \sim 1$  (and thus  $\omega\tau_2 \gg 1$ ) in which we recover (12),

$$\kappa \simeq \kappa_{HF} = \kappa_\infty + \frac{\kappa_i - \kappa_\infty}{1 + i\omega\tau_1}, \quad (18)$$

where HF stands for high frequency and a second one for  $\omega\tau_2 \sim 1$  (and  $\omega\tau_1 \ll 1$ ) in which we get

$$\kappa \simeq \kappa_{LF} = \kappa_i + \frac{\kappa_0 - \kappa_i}{1 + i\omega\tau_2}. \quad (19)$$

This is the low frequency approximation of  $\kappa$ . The low frequency limit of the high frequency incompressibility,  $\omega = 0$  in (18), is  $\kappa_i$  which of course is also the high frequency limit of the low frequency

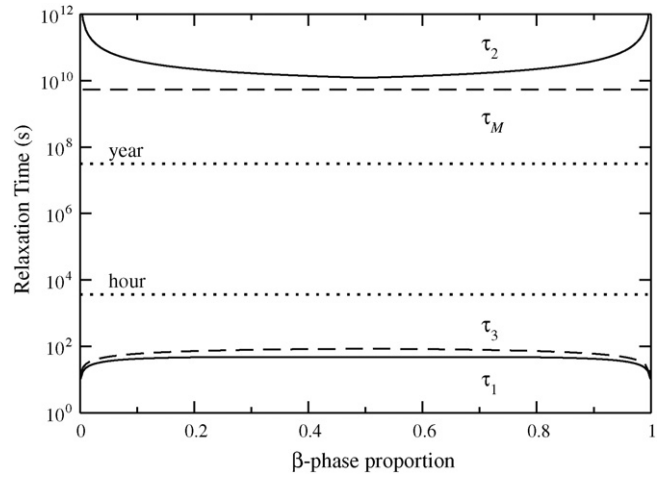


**Fig. 2.** Relaxation times of incompressibility ( $\tau_1$  and  $\tau_2$ ) and shear modulus ( $\tau_3$  and Maxwell time  $\tau_M$ ) across a phase loop. The two short relaxation times are in the seismic band of surface waves, for the bulk attenuation  $\tau_1$  and the shear attenuation  $\tau_3$ . The long bulk and shear relaxation times  $\tau_2$  and  $\tau_M$  correspond to viscoelastic behaviours occurring after at least one Maxwell time. The horizontal lines correspond to periods of 1 h and 1 yr (frequencies of 0.27 mHz and 0.03  $\mu$ Hz).

incompressibility,  $\omega = +\infty$  in (19). In other words, the intermediate incompressibility  $\kappa_i$  that we considered as relaxed with respect to the short time scale of phase change can in turn be seen as unrelaxed with respect to the large time scale of viscous flow.

Using experiments of Kubo et al. (1998) on growth of wadsleyite from olivine at 13.5 GPa and 1300 K, Morris (2002) suggests that the kinetic constant is  $C = 45 \text{ nm s}^{-1} \text{ GPa}^{-1}$ . Although it is not obvious to derive a value of  $C$  from the paper of Li and Weidner (2008), they mention reaction lengths of a few  $\mu\text{m}$ , in  $\sim 1 \text{ h}$ , for pressure offsets of  $\sim 0.1 \text{ GPa}$  which, within one order of magnitude, corresponds to the same range of kinetic constant. We choose a Maxwell time of  $\tau_M = 174 \text{ yr}$  corresponding to a viscosity of  $10^{21} \text{ Pa s}$ , and a radius  $R_e$  corresponding to the average distance between grains equal to 1 mm.

We show in Fig. 2 the evolution of the time constants  $\tau_1$  to  $\tau_2$  across the phase change. The volume ratio of  $\beta$ -phase across the loop varies more or less linearly with depth. The time constants are

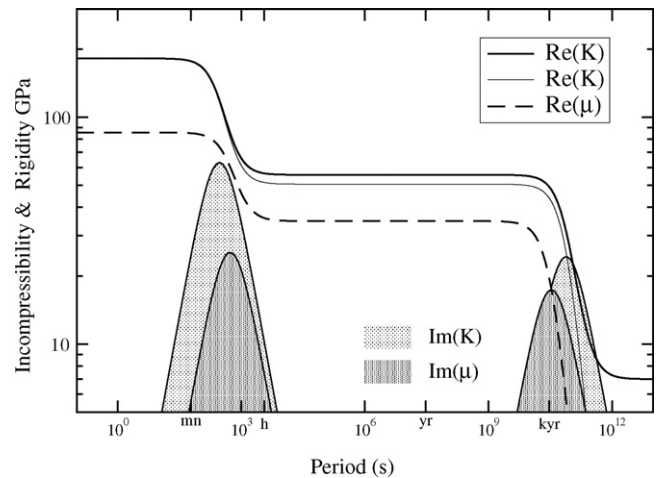


**Fig. 3.** Incompressibility and rigidity as functions of the period. The real part is depicted by lines, the imaginary part by shadows. The thin line corresponds to the incompressibility computed using (6), the thick line using (7). In the former case the incompressibility goes to zero at long period while in the latter, it reaches the relaxed compressibility  $\kappa_0$ . The high frequency relaxation occurs for seismic and tidal periods.

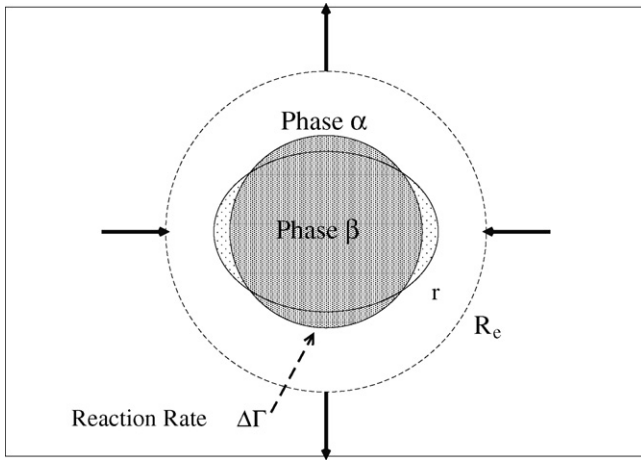


**Fig. 4.** To compute the shear attenuation, we submit the two-phase to a pure shear experiment. The pressure remains constant, but the high pressure  $\beta$ -phase starts growing in the direction of the maximum stress, the  $\alpha$ -phase in the direction of the lowest stress as the reaction rate is related to the normal stress on interfaces.

assumed symmetrical with respect to the vertical axis,  $S^3 = 1/2$  (we assume that the minor phase is always in the inner sphere; the  $\beta$ -phase proportion is thus  $S^3$  until a proportion of 50%,  $1 - S^3$  after). They do not vary much across the phase transition except when a phase is in a very small proportion. The short time constants for incompressibility relaxation  $\tau_1$  is lower than 48 s. The long time constant  $\tau_2$  is larger than the Maxwell time  $\tau_M$ .

Fig. 3 depicts the evolution of the real and imaginary part of the incompressibility in the middle of the phase loop ( $S^3 = 1/2$ ). The kinetic laws (6) and (7) have been used for the results of  $\text{Re}(\kappa)$  depicted with thick and thin lines, respectively. The two curves are very similar for short periods where the elastic incompressibility is recovered. They differ at long periods where the equilibrium in the loop imposes a relation between density and pressure given by the incompressibility  $\kappa_0$ . For intermediate periods, the phase change is inhibited by the elastic stresses controlled by the rigidity. The relaxation occurs in two steps over two different time ranges. During the high frequency relaxation, the reaction is limited by the elastic support that protects the minor phase. The reaction is controlled by diffusion and viscous relaxation at low frequency.

### 3. Pure shear deformation and complex rigidity

The existence of a phase change has also an effect on the rigidity. When at uniform pressure, the stresses are not uniform, the high pressure phase grows in the direction of the maximum stress and the reverse reaction occurs in the perpendicular direction (Fig. 4). This eases the deformation and therefore reduces the effective rigidity. Notice that it is only because the chemical potential in solids is related to the normal stress not to the pressure (uniform in a pure shear deformation) than reactions occur.

An analytical expression can be obtained, although the derivation is more cumbersome and less rigorous than in the spherical case. Let us consider the deformation of a nucleus of  $\beta$ -phase surrounded by a shell of  $\alpha$ -phase when a pure shear deformation is applied to the external boundary. The pure shear deformation far from the central nucleus is in cartesian coordinates  $u_z = -\gamma z$ ,  $u_x = \gamma x/2$  and  $u_y = \gamma y/2$  ( $\gamma$  is the strain) and can be written in spherical coordinates after a standard change of coordinates

$$u_r = -\frac{1}{2}\gamma r(3 \cos^2 \theta - 1), \quad \text{and} \quad u_\theta = \frac{3}{2}\gamma r \cos \theta \sin \theta, \quad (20)$$

where  $\theta$  is the colatitude.

In a pure shear experiment performed in a laboratory, the rigidity would be the ratio between the vertical stress applied on the surface of a core sample, at position  $z$ , and the vertical strain measured at the same position  $-z\sigma_{zz}(z)/2u_z(z)$ . In our analytical model, instead of imposing the deformation on surfaces of constant cartesian coordinates, they are imposed on the sphere or radius  $R_e$ . We consider that the effective rigidity can however be estimated by

$$\mu = -\frac{\sigma_{rr}(R_e, \theta)R_e}{2u_r(R_e, \theta)}. \quad (21)$$

We can solve for the deformation inside the two-phase aggregate by assuming that it keeps the same degree 2 geometry. As the radial stress and the radial deformation have the same geometry,  $\mu$  is independent of  $\theta$ . In this case, the general solution of the momentum balance yields

$$u_r^i = \left( a_i s + b_i s^3 + \frac{c_i}{s^2} + \frac{d_i}{s^4} \right) (3 \cos^2 \theta - 1) \quad (22)$$

and

$$u_\theta^i = \left( -3a_i s - b_i \frac{7\mu + 5\lambda_\infty}{\lambda_\infty} s^3 - 6 \frac{\mu_\infty}{3\lambda_\infty + 5\mu} \frac{c_i}{s^2} + 2 \frac{d_i}{s^4} \right) \cos \theta \sin \theta \quad (23)$$

where  $s$  is again the normalized radius  $s = r/R_e$ ,  $\lambda_\infty = K_\infty - 2\mu_\infty/3$  is an elastic Lamé parameter, and  $i$  stands for  $\alpha$  or  $\beta$ .

Using (22) and (23), the stress tensor can be computed in the inner sphere and in the outer shell (see Appendix B). The final resolution involves the determination of six parameters  $a_\alpha, b_\alpha, c_\alpha, d_\alpha, a_\beta$  and  $b_\beta$ . They can be obtained by matching six boundary conditions; the continuity of shear stress, normal stresses and tangential deformation on the interface, the jump condition for the normal velocity on the interface, and the two external boundary conditions (20) (see Appendix B). Notice that no density variation occurs in the assemblage submitted to a pure shear and the kinetic law (6) is therefore appropriate. Similarly to what we obtain for the incompressibility, the effective rigidity deduced from the model can be written as

$$\mu_{HF} = \mu_\infty + \frac{\mu_i - \mu_\infty}{1 + i\omega\tau_3}. \quad (24)$$

where the intermediate rigidity  $\mu_i$  is

$$\mu_i = \mu_\infty - \mu_\infty F \left( S, \frac{\kappa_\infty}{\mu_\infty} \right), \quad (25)$$

where  $F$  is a cumbersome function of  $S$  and  $\kappa_\infty/\mu_\infty$ . We can choose for simplicity  $\kappa_\infty = 5\mu_\infty/3$  which corresponds to a Poisson ratio of 1/4 (or to the equality of the two Lamé Parameters  $\lambda_\infty$  and  $\mu_\infty$  (e.g., Malvern, 1969)) which is a common rule of thumb for elasticity of silicates. In this case, the function  $F$  is

$$F \left( S, \frac{\kappa_\infty}{\mu_\infty} = \frac{5}{3} \right) = 105S^3 \frac{8 + S^2}{604 + 280S^3 + 56S^5 + 5S^7}, \quad (26)$$

and the relaxation times  $\tau_3$  is

$$\tau_3 = 315 \frac{SR_e}{C\mu_\infty} \frac{1}{604 + 280S^3 + 56S^5 + 5S^7}. \quad (27)$$

The constant  $\tau_3$  of shear modulus relaxation is also depicted in Fig. 2 and its value is comparable to that appearing in the high frequency incompressibility  $\tau_2$ .

Like for the incompressibility, the intermediate rigidity  $\mu_i$  that corresponds to the relaxed limit of the rigidity with respect to the short time scale of phase change can in turn be seen as an unrelaxed rigidity for periods larger than  $\tau_3$  but much smaller than the Maxwell time. Replacing directly in (24) and (25),  $\mu_\infty$  by  $\mu^*$ , see (15), is straightforward but leads to a very complex expression of  $\mu$ . We checked numerically that the behavior of  $\mu^*F(\kappa_\infty/\mu^*)$  can

be qualitatively approximated by  $\mu^*F(\kappa_\infty/\mu_\infty)$ . For periods much larger than  $\tau_3$ , the rigidity varies therefore as

$$\mu = \left( \mu_\infty + \frac{\mu_i - \mu_\infty}{1 + i\omega\tau_3} \right) \frac{i\omega\tau_M}{1 + i\omega\tau_M}. \quad (28)$$

As  $\tau_3 \ll \tau_M$ , the expression of the rigidity at high frequency, when  $\omega\tau_M \gg 1$  is  $\mu \simeq \mu_{HF}$ . At low frequency, when  $\omega\tau_3 \ll 1$  we get

$$\mu \simeq \mu_{LF} = \mu_i - \frac{\mu_i}{1 + i\omega\tau_M}, \quad (29)$$

which reaches zero after complete relaxation when  $\omega = 0$ , i.e., when the medium behaves viscously rather than elastically.

The real and imaginary parts of the rigidity are plotted in Fig. 3. Like for the incompressibility, two transitions are predicted. The low frequency transition only occurs when the elastic stresses in the surrounding shell relax and stop screening the inner nucleus from the outside stresses. At zero frequency (infinite period), the rigidity vanishes contrary to the incompressibility that remains finite.

#### 4. Bulk and shear attenuations

In the case of complex elastic parameters, the seismic waves propagates with a frequency-dependent attenuation usually defined by the quality factors  $Q_\xi$  where  $\xi$  stands for  $\kappa$  or  $\mu$ . These quality factors are defined by

$$Q_\xi = -\frac{\text{Re}(\xi)}{\text{Im}(\xi)} = \frac{\xi^R + \xi^U \omega^2 T_R^2}{(\xi^U - \xi^R)\omega T_R}, \quad (30)$$

where  $T_R$  is the appropriate relaxation time,  $\text{Re}(\xi)$  and  $\text{Im}(\xi)$  the real and imaginary parts of  $\xi$  that varies between the relaxed and unrelaxed limits,  $\xi^R$  (for  $\omega = 0$ ) and  $\xi^U$  (for  $\omega = +\infty$ ). Attenuation is maximum at the frequency

$$\omega_0 = \frac{1}{T_R} \sqrt{\frac{\xi^R}{\xi^U}}, \quad (31)$$

where  $Q_\xi$  reaches its minimum

$$Q_\xi^0 = 2 \sqrt{\frac{\xi^R \xi^U}{\xi^U - \xi^R}}. \quad (32)$$

Notice that in our model, each elastic parameter has low and high frequency modes. The bulk modulus can relax from  $\xi^U = \kappa$  to  $\xi^R = \kappa_i$  with the time constant  $\tau_1$ , then from  $\xi^U = \kappa_i$  to  $\xi^R = \kappa_0$  with the time constant  $\tau_2$ . Similarly, the rigidity relaxes from  $\xi^U = \mu$  to  $\xi^R = \mu_i$  with the time constant  $\tau_3$ , then from  $\xi^U = \mu_i$  to  $\xi^R = 0$  with the time constant  $\tau_M$ .

Fig. 5 depicts the minimum quality factor  $Q_\kappa^0$  and  $Q_\mu^0$  for the various relaxation times and across the two-phase loop. Like for Fig. 2, we assume that our model is valid until  $S^3 = 1/2$ , then swap the roles of the minor and major phases, which simply symmetrises the results with respect to the middle of the loop. Values lower than 10 are predicted for the high frequency bands. The bulk attenuation in the coexistence loop observed by Li and Weidner (2008) is indeed found maximum when the two phases are in similar proportions, as predicted by our model. To compute the bulk attenuation, we use either a  $\kappa_0$  deduced from the thickness of the phase change (thick line, see Eq. (7)) or  $\kappa_0 = 0$  (thin line, see (6)). This does not really change the predicted quality factor. The low frequency bulk attenuation is very low but corresponds to very long time constants not relevant to seismology as seen in Fig. 6.

Fig. 6 depicts the attenuation quality factor  $Q_\kappa$  and  $Q_\mu$  computed at the center of the phase loop ( $S^3 = 1/2$ ) as a function of the period of the excitation. The solid lines correspond to the bulk attenuation, the dashed line to the shear attenuation. A minimum of quality factors is predicted for frequencies between 0.27 and 16 mHz (periods

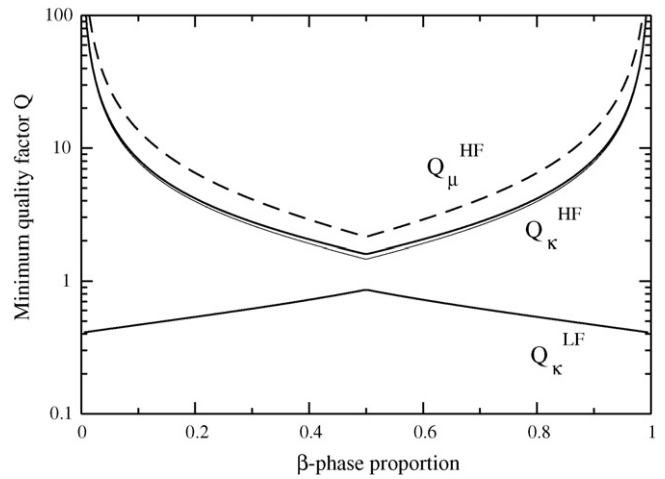


Fig. 5. Evolution of the quality factor across the phase change. The volume proportion of the high pressure phase varies more or less linearly with depth with across the phase change. The high frequency quality factor for both  $Q_\kappa^0$  and  $Q_\mu^0$  are below 10 in the center of the loop. The exact value of  $\kappa_0$  ( $7 \times 10^9$  GPa, thick solid line, or 0, thin solid line) is not very important. The very low quality factor of  $Q_\kappa^0$  at low frequency does not belong to the seismic or tidal domain.

between 1 min and 1 h). At very low frequencies, when the mantle behaves viscously, the quality factors become also very low. Assuming a zero  $\kappa_0$  or a finite  $\kappa_0$  is only visible at very long periods: the phase loop maintains a finite compressibility (thick line) in the latter case, but cannot resist compression (thin line) in the former case. The shear quality factor reaches zero at zero frequency where the mantle behaves viscously rather than elastically. The general behavior for the shear attenuation is that of a linear solid called a Burger body (see e.g., Karato and Spetzler, 1990). The bulk attenuation behaves differently as contrary to the Burger body, the quality factor does vanish at infinite periods.

The fact that the bulk quality factor is lower than the shear quality factor is not a general result of our model. The difference  $\kappa_i - \kappa_\infty$  that controls the bulk attenuation is proportional to  $\kappa_0 - \kappa_\infty$  (see (12) and (13)). This difference tend to decrease when the loop thickness increases (see (3)). On the contrary the difference  $\mu_i - \mu_\infty$  controlling the shear attenuation is independent of the loop thickness (see (24)). The ratio  $Q_\kappa/Q_\mu$  decreases therefore with the loop thickness. Increasing the loop thickness over 50 km for the 410 km

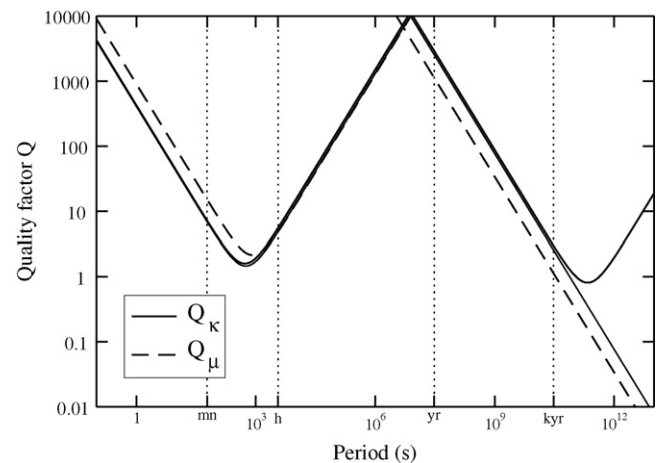
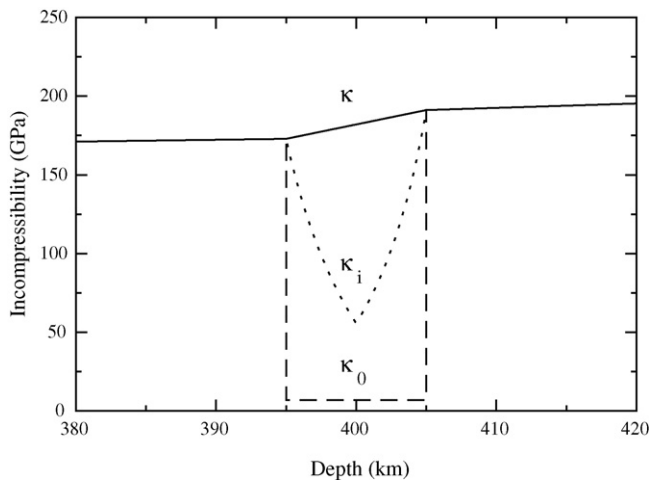


Fig. 6. Quality factors at the middle of the phase loop, as a function of the period of the excitation. Two attenuation bands are predicted, one between 1 min and 1 h (from 16 to 0.27 mHz) the other for times larger than the Maxwell time. The minima correspond to the extrema depicted at the middle of the phase loop in Fig. 5. The thin line corresponds to the value of  $Q_\kappa$  computed with  $\kappa_0 = 0$ .



**Fig. 7.** Various incompressibilities have been defined in this paper within a two-phase coexisting zone. The elastic incompressibility  $\kappa$ , seen by high frequency body waves, the totally relaxed compressibility  $\kappa_0$  that can be deduced from the density jump and the thickness of the transition, and an intermediate incompressibility  $\kappa_i$ , see Eq. (13). The transition between  $\kappa$  and  $\kappa_i$  and an associated attenuation should occur for periods corresponding to surface waves. The transition between  $\kappa_i$  and  $\kappa_0$  should take a much longer time (a Maxwell time larger than 100 yr).

transition (keeping the other parameters unchanged) would lead to  $Q_\mu$  lower than  $Q_\kappa$ . In other words, a thin loop is mostly attenuating because of its  $Q_\kappa$ , a thick one because of its  $Q_\mu$ .

## 5. Conclusions

Our model of attenuation in coexistence loop is certainly simplified in particular in the description of the geometry of the two phases. However we believe that various aspects of our model are very robust.

We confirm that the phase loops, in agreement with Li and Weidner (2008) should be the location of a significant attenuation for periods belonging to the low frequency seismic band (surface waves and seismic modes). However in their paper, only the bulk attenuation was taken into account whereas we have shown that the shear attenuation should be affected as well. Moreover, we found that the two attenuations and their relaxation times are independent of the amplitude of the seismic wave in agreement with the usual assumption of seismology. The attenuation bands are narrow because of our assumption of a unique grainsize across the coexistence loop. A distribution of grainsizes would probably broaden the frequency bands of attenuation.

Another large difference between Li and Weidner (2008) and the present paper is that the transition between the elastic incompressibility,  $\kappa_\infty$  and that deduced from PREM  $\kappa_0$  (very low incompressibility in coexistence loops) does not occur in a single step but in two steps. This is summarized in Fig. 7 where we plot as a function of depth the instantaneous  $\kappa_\infty$ , the intermediate  $\kappa_i$  and the  $\kappa_0$  bulk moduli. We derived a  $\kappa_\infty(r)$  that follows the PREM values outside the loop and varies linearly within the loop. We introduce the same  $\kappa_\infty(r)$  in the computation of  $\kappa_i$ , (13). These depth-dependent incompressibilities look more realistic, but truly our model assumes the  $\kappa_\infty$  is uniform within the loop. We predict that the transformation is first limited by the shielding of the external stresses by the elastic rigidity of the matrix. This behavior is in agreement with Morris (2002). This first “fast” transition between  $\kappa_\infty$  and  $\kappa_i$  (see Fig. 7) occurs within minutes or hours. Therefore the incompressibility seen by seismology is somewhere between these two values. The final transformation (slow kinetics) corresponding to the transition between  $\kappa_i$  and  $\kappa_0$  occurs in a second step when the elastic stresses are released, and a new two-phase equilibrium

is found after diffusion and reequilibration of the composition. A very similar figure could be drawn for the rigidity, but the totally relaxed rigidity would simply be zero.

The minimum values of  $Q_\kappa$  and  $Q_\mu$  predicted for the olivine–wadsleyite loop are significantly lower than the typical range of attenuation of low frequency seismologic models. This is true for the shear attenuation and even more for the bulk attenuation. In a recent review, Resovsky et al. (2005) propose for depths around 400 km a  $Q_\mu$  roughly between 150 and 200 and  $Q_\kappa$  larger than 2000. These radial models have used a very simple parametrization of the attenuation in a limited range of layers (typically larger than 200 km) and in layers than coincide with the seismic discontinuities. This parametrization is certainly an inappropriate choice to detect a narrow depth range of attenuation astride a velocity discontinuity.

The  $Q_\kappa$  and  $Q_\mu$  quality factors seen by given seismic or tidal perturbations are not necessary the minimum values shown in Figs. 5 and 6, but are functions of their frequencies, of the kinetic constant  $C$  and of the grain size  $R_e$ . The exact frequency dependent expressions for incompressibility, rigidity and attenuation can be easily computed from (12), (24) and (30). The values of  $C$  and  $R_e$  are still uncertain for the olivine–wadsleyite phase change and mostly unknown for other mantle phase changes. The narrow depth range of the coexistence loop,  $\sim 10$  km, may make this localized attenuation difficult to detect but may significantly bias the average determined over a large zone of sensibility. The presence of bulk attenuation in the upper mantle has indeed be proposed by various studies (Resovsky et al., 2005; Durek and Ekstrom, 1996).

The existence of a strong attenuation associated with seismic velocity jumps should also affect the reflection and transmission factors of short period seismic waves hitting these interfaces. Notice however that body waves seem to have a too high frequency to be right on the attenuation maximum, but according to Fig. 6 might see an attenuation of order 10–100 (for frequencies between 1 Hz and 20 mHz). This could possibly be seen from S waves multiply reflected under the Earth surface and with a turning point below or above the 410 km discontinuity. At any rate, a better estimate of attenuation in phase loops would constrain the kinetic behavior of these phase changes (Chambat et al., 2009).

We have discussed the attenuation due to the olivine–wadsleyite transition because this transition is simple and only involves two phases of similar composition. Other mantle transitions should behave similarly like the wadsleyite–ringwoodite loop around 520 km deep (but, of course, with their appropriate kinetic laws that may not lead to characteristic times for the phase changes in tune with the seismic periods). The mantle transitions involving three phase like the ringwoodite to ferropericlasite + perovskite, should also lead to attenuation because of a large difference between the relaxed and unrelaxed properties. However because of the necessary long distance motion of atoms during the transformation, a model of kinetics seems yet difficult to propose.

## Acknowledgments

This work has been supported by the CNRS-INSU Dyeti program. We thank Tine Thomas for interesting discussions on seismic attenuation.

## Appendix A. Radial deformation

The deformation given by (8) corresponds to the radial stress

$$\sigma_{rr}^i = 3\kappa \frac{a_i}{R_e} - 4\mu \frac{b_i}{R_e s^3}. \quad (\text{A.1})$$

The continuity of normal stress across the phase transition boundary satisfies

$$3\kappa a_\alpha - 4\mu b_\alpha \frac{1}{s^3} = 3\kappa a_\beta, \quad (\text{A.2})$$

while the application of an external pressure corresponds to

$$3\kappa \frac{a_\alpha}{R_e} - 4\mu \frac{b_\alpha}{R_e} = -\delta P. \quad (\text{A.3})$$

The condition of jump of normal displacement where the phase change occurs is

$$i\omega \left( a_\alpha s + \frac{b_\alpha}{s^2} - a_\beta s \right) = C \left( 3\kappa \frac{a_\beta}{R_e} + \frac{\kappa_0}{\kappa_v} \delta P \right). \quad (\text{A.4})$$

The resolution of Eqs. (A.2)–(A.4) leads to the unknowns  $a_\alpha$ ,  $b_\alpha$  and  $a_\beta$  and therefore to the expression of the effective incompressibility (see (10))

$$\kappa = -\frac{R_e}{3(a_\alpha + b_\alpha)} \delta P. \quad (\text{A.5})$$

## Appendix B. Pure shear deformation

From expressions (22) and (23), stresses can then be readily obtained,

$$\sigma_{rr}^i = \frac{\mu}{R_e} \left( 2a_i - b_i s^2 - 2 \frac{9\lambda_\infty + 10\mu_\infty}{3\lambda_\infty + 5\mu_\infty} \frac{c_i}{s^3} - 8 \frac{d_i}{s^5} \right) (3 \cos^2 \theta - 1), \quad (\text{B.1})$$

$$\sigma_{r\theta}^i = -2 \frac{\mu}{R_e} \left( 3a_i + \frac{8\lambda_\infty + 7\mu_\infty}{\lambda_\infty} b_i s^2 + 3 \frac{3\lambda_\infty + 2\mu_\infty}{3\lambda_\infty + 5\mu_\infty} \frac{c_i}{s^3} + 8 \frac{d_i}{s^5} \right) \cos \theta \sin \theta, \quad (\text{B.2})$$

where  $i$  stands for  $\alpha$  or  $\beta$ .

To avoid unnecessary complexities, we assume  $\lambda_\infty = \mu_\infty$  or  $\kappa_\infty = 5\mu_\infty/3$ . This time, the boundary conditions on the outer shell imply

$$a_\alpha + b_\alpha + c_\alpha + d_\alpha = -\frac{\gamma}{2}, \quad (\text{B.3})$$

$$\frac{1}{4}(-12a_\alpha - 48b_\alpha - 3c_\alpha + 8d_\alpha) = \frac{3\gamma}{2}, \quad (\text{B.4})$$

the continuity of radial and shear stress at the phase-change interface implies

$$\left( 8a_\alpha - 4b_\alpha s^2 - 19 \frac{c_\alpha}{s^3} - 32 \frac{d_\alpha}{s^5} \right) = (8a_\beta - 4b_\beta s^2), \quad (\text{B.5})$$

$$-\left( 24a_\alpha + 120b_\alpha s^2 + 15 \frac{c_\alpha}{s^3} + 64 \frac{d_\alpha}{s^5} \right) = -(24a_\beta + 120b_\beta s^2), \quad (\text{B.6})$$

and the continuity of  $\theta$ -displacement

$$\frac{1}{4} \left( -12a_\alpha s - 48b_\alpha s^3 - 3 \frac{c_\alpha}{s^2} + 8 \frac{d_\alpha}{s^4} \right) = \frac{1}{4} (-12a_\beta s - 48b_\beta s^3). \quad (\text{B.7})$$

As there is no global volume change in this pure shear experiment the jump of radial displacement is given by (6)

$$i\omega \left( \left( a_\alpha s + b_\alpha s^3 + \frac{c_\alpha}{s^2} + \frac{d_\alpha}{s^4} \right) - (a_\beta s + b_\beta s^3) \right) = C \frac{1}{4} \frac{\mu_\infty}{R_e} (8a_\beta - 4b_\beta s^2). \quad (\text{B.8})$$

The resolution of Eqs. (B.3)–(B.8) leads to the unknowns  $a_\alpha$ ,  $b_\alpha$ ,  $c_\alpha$ ,  $d_\alpha$ ,  $a_\beta$  and  $b_\beta$ . At last, we estimate the effective shear modulus according to (21)

$$\mu = \frac{\mu_\infty}{4} \frac{8a_\alpha - 4b_\alpha - 19c_\alpha - 32d_\alpha}{a_\alpha + b_\alpha + c_\alpha + d_\alpha}. \quad (\text{B.9})$$

## References

- Aki, K., Richards, P.G., 2002. Quantitative Seismology. University Science Books, New York.
- Anderson, D.L., 1976. The earth as a seismic absorption band. *Science* 196, 1104–1106.
- Anderson, D.L., Given, J.W., 1982. Absorption-band q model for the earth. *J. Geophys. Res.* 87, 3893–3904.
- Brodholt, J.P., Hellfrich, G., Trampert, J., 2007. Chemical versus thermal heterogeneity in the lower mantle: the most likely role of anelasticity. *Earth Planet. Sci. Lett.* 262, 429–437.
- Bullen, K.E., 1940. The problem of the earth's density variation. *Seismol. Soc. Am. Bull.* 30, 235–250.
- Chambat, F., Durand, S., Matas, J., Ricard, Y., 2009. Constraining the kinetics of mantle phase changes with seismic mode data. *Earth Planet. Sci. Lett.*, in preparation.
- de Groot, S.R., Mazur, P., 1984. Non-Equilibrium Thermodynamics. Dover Publications, New York.
- Durek, J., Ekstrom, G., 1996. A radial model of anelasticity consistent with long-period surface wave data. *Bull. Seismol. Soc. Am.* 86, 144–158.
- Dziewonski, A.M., Anderson, D., 1981. Preliminary reference earth model. *Phys. Earth Planet. Inter.* 25, 297–356.
- Gung, Y., Romanowicz, B., 2004. Q tomography of the upper mantle using three-component long-period waveforms. *Geophys. J. Int.* 157, 813–830.
- Jacobs, M.H.G., de Jong, B.H.W.S., 2005. An investigation into thermodynamic consistency of data for the olivine, wadsleyite and ringwoodite form of  $(\text{Mg,Fe})_2\text{SiO}_4$ . *Geochim. Cosmochim. Acta* 69, 4361–4375.
- Jackson, D.D., Anderson, D.L., 1970. Physical mechanisms of seismic-wave attenuation. *Rev. Geophys. Space Phys.* 8, 1–63.
- Jackson, I., 2007. Physical origins of anelasticity and attenuation in rock. In: Schubert, G. (Ed.), *Treatise of Geophysics*. Vol. 2. Mineral Physics: Properties of Rocks and Minerals. Elsevier Scientific Publishing Company, New York, pp. 496–522 (Chapter 2.17).
- Karato, S., Spetzler, H.A., 1990. Defect microdynamics in minerals and solid-state mechanisms of seismic-wave attenuation and velocity dispersion in the mantle. *Rev. Geophys.* 28, 399–421.
- Karato, S.I., Karki, B.B., 2001. Origin of lateral variation of seismic wave velocities and density in the deep mantle. *J. Geophys. Res.* 106, 21771–21783.
- Krien, Y., Fleitout, L., 2008. The accommodation of volume changes in phase transition zones: implications for mantle dynamics and metamorphism. *J. Geophys. Res.* in preparation.
- Kubo, T., Ohtani, E., Shinmei, T., Fujino, K., 1998. Effects of water on the  $\alpha$ - $\beta$  transformation kinetics in San Carlos olivine. *Science* 281, 85–87.
- Lekić, V., Matas, J., Panning, M., Romanowicz, B., 2009. *Earth and Planet. Sci. Lett.* 282, 285–293.
- Li, L., Weidner, D.J., 2008. Effect of phase transitions on compressional-wave velocities in the earth's mantle. *Nature* 454, 984–986.
- Malvern, L., 1969. *Introduction to the Mechanics of a Continuum Medium*. Prentice-Hall Series in Engineering of the Physical Sciences.
- Matas, J., Bukowinski, M.S.T., 2007. On the anelastic contribution to the temperature dependence of lower mantle seismic velocities. *Earth Planet. Sci. Lett.* 259, 51–65.
- Morris, S.J.S., 2002. Coupling of interface kinetics and transformation-induced strain during pressure-induced solid-solid phase changes. *J. Mech. Phys. Solids* 50, 1363–1395.
- Paterson, M.S., 1973. Non hydrostatic thermodynamics and its geological applications. *Rev. Geophys.* 11, 355–389.
- Resovsky, J., Trampert, J., van der Hilst, R.D., 2005. Error bars for the global q profile. *Earth Planet. Sci. Lett.* 230, 413–423.
- Ricard, Y., 2007. Physics of mantle convection. In: Schubert, G. (Ed.), *Treatise of Geophysics*. Vol. 7. Mantle Dynamics of Treatise on Geophysics. Elsevier Scientific Publishing Company, New York, pp. 31–87 (Chapter 7.02).
- Ricard, Y., Mattern, E., Matas, J., 2005. Mineral physics in the thermodynamic mantle models. In: Hilst, R., et al. (Eds.), *Composition, Structure and Evolution of the Earth Mantle*. Vol. AGU Monograph 160, pp. 283–300.
- Ringwood, A., 1982. Phase transformations and differentiation in subducted lithosphere: implications for mantle dynamics, basalt petrogenesis, and crustal evolution. *J. Geol.* 90 (6), 611–642.
- Romanowicz, B., Mitchell, B., 2007. Q in the earth from crust to core. In: Schubert, G. (Ed.), *Treatise of Geophysics*. Vol. 1. Seismology and Structure of the Earth of Treatise on Geophysics. Elsevier Scientific Publishing Company, New York, pp. 731–774 (Chapter 1.21).
- Rubie, D., Ross, C.R., 1994. Kinetics of the olivine-spinel transformation in subducting lithosphere: experimental constraints and implications for deep slab processes. *Phys. Earth Planet. Inter.* 86, 223–241.
- Shearer, P.M., 2000. Upper mantle seismic discontinuities. In: Karato, S., et al. (Eds.), *Earth's Deep Interior: Mineral Physics and Tomography from the Atomic to the Global Scale*. Vol. AGU Monograph 117, pp. 115–131.
- Shimizu, I., 1997. The non-equilibrium thermodynamics of intracrystalline diffusion under non-hydrostatic stress. *Philos. Mag. A* 75, 1221–1235.
- Van der Meijde, M., Marone, M., Giardini, D., van der Lee, S., 2003. Seismic evidence for water deep in earth's upper mantle. *Science* 300 (doi: 10.1126/science.1083636).
- Widmer, R., Masters, G., Gilbert, F., 1991. Spherically symmetric attenuation within the earth from normal mode data. *Geophys. J. Int.* 104, 541–553.